A high density composite fuel with integrated burnable absorber: U3Si2-UB2

Turner, Joel; Middleburgh, Simon; Abram, Tim

Journal of Nuclear Materials

Published: 01/02/2020

Peer reviewed version

A high density composite fuel with integrated burnable absorber: U_3Si_2-UB_2

J. Turner[1], S.C. Middleburgh[2], T.J. Abram[1]

[1]*Nuclear Fuel Centre of Excellence, The University of Manchester, United Kingdom*

[2]*Nuclear Futures: Materials, Bangor University, Bangor, LL57 1UT, United Kingdom*

Abstract

UB_2-U_3Si_2 composite fuel pellets have been manufactured and characterised. Both main phases were observed to be stable in contact with one-another up to the maximum processing temperature of 1500°C. The solubility and behaviour of hydrogen in UB_2 was predicted and compared to previous work on the gas' behaviour in U_3Si_2. H_2 was found to be insoluble in UB_2 to any great extent, a clear distinction to the behaviour with U_3Si_2.

Keywords: Nuclear, Accident Tolerant Fuel, Burnable Absorber

1. Introduction

The nuclear accident at Fukushima Diachii has lead to extensive research into so-called Accident Tolerant Fuels (ATFs). These new combinations of fuel and cladding materials aim to offer significant advantages over the current UO_2 fuel and zirconium cladding materials used predominantly in light water reactors. Potential advantages of the new systems include reduced fuel centre-line temperatures, higher power to melt ratios and improved oxidation performance under accident conditions with an associated reduction in hydrogen production.

A leading candidate ATF system is U_3Si_2 fuel pellets within a silicon carbide or chromium coated zirconium-alloy cladding. This has been the subject of considerable recent academic and industrial interest, which has culminated in a series of test irradiations at the Idaho National Laboratory [1, 2]. U_3Si_2 has a higher uranium density than UO_2, and an improved thermal conductivity. In concert with an advanced cladding solution such as SiC, it therefore offers both economic and safety advantages over UO_2/zirconium. However, recent results suggest that the performance of U_3Si_2 in high temperature steam may be unacceptable, leading to the energetic pulverisation of the fuel pellet and rapid oxidation resulting in severe fuel failure [3].

This rapid pulverisation is thought to be a result of the unexpectedly high volume change which occurs when U_3Si_2 reacts with hydrogen to form $U_3Si_2H_2$, experimentally observed and predicted by atomistic modelling to be around 10% [4, 5], resulting in a drastic increase in reactive surface area and further oxidation and hydrogen production. When considering steam reactions, hydrogen is formed from an initial oxidation reaction, and so in practice limiting either the oxidation or hydride-formation reactions could greatly improve steam performance in this fuel material.

UB_2 enriched in ^{11}B has been the source of burgeoning interest as a fuel material, as a result of its physical and neutronic properties. Recent modelling and experiment suggests that UB_2 may be a significant ATF candidate in its own right [6, 7, 8] with a uranium density of 11.6 g/cm^3 [9].

Furthermore, there remains the need to develop a burnable absorber (BA) concept for U_3Si_2 pellets. Gadolinium compounds have been shown to cause degradation of the U_3Si_2 phase, forming both uranium metal and USi phases; gadolinium is therefore not a credible candidate for homogeneous inclusion within U_3Si_2 [10].

One potential option is to utilise UB_2 as a BA within U_3Si_2. It is possible to vary the enrichment of ^{10}B such that the material will act as a BA in some core regions and a simple fuel in other regions.

Atomic scale modelling (Section 2.2) suggests that the addition of UB_2 to U_3Si_2 may both allow for reactivity control and may potentially inhibit a mechanism that leads to the adverse steam reaction observed by Sooby-Wood et al. [3], thus preventing or slowing the rapid pulverisation of the material.

2. Methodology

2.1. Fabrication Methodologies

The primary goal of the experimental trials conducted at Manchester was to demonstrate the feasibility of U_3Si_2/UB_2 composite materials under 'standard' sintering treatment. In this context, 'standard' refers to utilising similar powder preparation and sintering parameters to those employed in existing U_3Si_2 studies [1].

2.1.1. Arc Melting

Early trials of producing U_3Si_2-boron composites proceeded via the use of arc melting; combining elemental boron or a combination of elemental boron and silicon with U_3Si_2 and observing the material phases produced on cooling. Both methodologies produced similar results to previous work involving the arc melting of gadolinium with uranium silicide **??**, with the U_3Si_2 phase breaking down to form silicon rich regions, alongside the formation of a uranium metal phase. This programme was halted after a small number of trials, and cold pressing and sintering of composite discs was investigated for further trials.

2.1.2. Powder Production

In order to introduce UB_2 in a lower temperature and more controlled regime, UB_2 and U_3Si_2 powders were combined and used to produce small discs. UB_2 powder was produced by high energy ball milling an ingot of UB_2 produced directly from arc-melting uranium metal and elemental boron. During this process, crystalline boron was seen to react particularly energetically to the process, and often shattered preventing its inclusion within the arc melted button. As such, boron was added until the required mass was reached for stoichiometry, assuming no uranium was lost during the process. Uranium silicide powder was produced following the method detailed within [10].

Tungsten carbide milling vessels and media were required to successfully mill UB_2; the use of hardened steel tooling resulted in the impregnation of UB_2 into both the vessel and milling media and the loss of a large volume of material. To counteract this, 0.01 g polyethylene-glycol (PEG) was added to each 50 ml milling vessel for future runs, which proved successful with

tungsten carbide mills but made little difference to the performance of hardened steel milling media.

Previous experience at Manchester has shown that the age of U_3Si_2 powder can have a significant impact on the sintering performance of green pellets produced from it, assumed to be through the formation of a thin silicon oxide layer on the powder surface. This has been observed even in very low O_2 environments (<1 ppm O_2). As the powder employed in these preliminary studies was around two weeks old, it was expected that discs produced from this material would be of reasonably low density and show large volumes of porosity.

2.1.3. Cold Press and Sintering

Several composite mixtures were produced ranging from pure U_3Si_2 to pure UB_2. In order to observe phase instability when either U_3Si_2 or UB_2 was the dominant phase, 10 wt.% and 90 wt.% UB_2 mixtures were studied, as well as a 50 wt.% UB_2 mixture. Powder milling, mixing and pressing were all performed within an atmosphere controlled argon glovebox, typically less than 1 ppm O_2.

Powders were mechanically mixed by hand to maintain the stoichiometry of the desired mixtures, as it was observed during milling that each compound behaved differently within stainless steel and tungsten carbide milling vessels. U_3Si_2 behaves well in stainless steel, but a large fraction becomes unrecoverable within tungsten carbide vessels. UB_2 responds in the opposite fashion. Hence hand mixing via rolling and shaking within a quartz vessel was used to blend the powders. This occasionally resulted in variations in local stoichiometry between the different uranium phases, particularly the 50 wt.%-50 wt.% mixture of UB_2 and U_3Si_2. It proved relatively easy to identify these regions and remove them from further analysis, as they showed a significantly altered microstructure.

Powders were pressed into 6mm diameter discs using a mechanical press to a pressure of 120 MPa. Die tooling was lubricated with zinc stearate to ease sample removal. Green discs all appeared to be well formed, although on handling with tweezers some damage occurred, particularly around the circumference of pellets. This was not unexpected given the use of milling lubricant, and did not prevent the use of these samples for further testing within this work. Later pellets were produced with a small mix of binding agent (PolyOx[1]) which greatly improved green pellet robustness.

Composite and U_3Si_2 pellets were sintered within graphite crucibles utilising a graphite-lined vacuum furnace. Tantalum beads and foil were used to limit contact between fuel materials and graphite, as well as acting as an oxygen getter during sintering. Vacuum was maintained at at least 10^{-3} mbar during sintering. Pellets were held at 1500 °C for one hour, with shorter isothermal steps at 350 °C and 650 °C to remove remaining PEG and binder material. Pure UB_2 pellets were sintered with a maximum temperature of 1800 °C, with a one hour hold time.

Sintered pellets were partially friable, as expected due to the age of the silicide powder employed, and had a relatively low density compared to typical targets for fuel: approximately 70-80%. This large range in density is due to the non-standard geometry produced during the process, and the difficulty in employing pycnometry or immersion density measurements to porous materials. Density measured by pycnometry was high (above 90%) indictating a large volume of open porosity, consistent with gas evolution during the sintering stage. UO_2 is typically sintered with a target density of 95% of theoretical density, which is also a general target for sintered

[1] Polyethylene Oxide M.W. 100,000

U_3Si_2 in order to accomodate fission induced swelling of the fuel and hence reduce the strain in the cladding [11]. The pellets produced here were significantly below this value. This was not considered problematic for the current study, as microstructural examination and phase identification (Section 3.1) could still be conducted without issue, and both reference silicide and composite materials appeared to be broadly similar in sintering behaviour.

2.2. Atomic Scale Modelling

Density functional theory based calculations were performed at Bangor University using the Vienna Ab-initio Software Package (VASP) [12, 13, 14]. Projector augmented-wave potentials [15] were used with the GGA-PBE exchange correlation [16] supplied with the software.

Simulations of UB_2 were performed using a 4×4×3 super-cell of the *P*6/*mmm* unit-cell (similar to previous work on the ZrB_2 system [17]). A 4×4×4 gamma centred *k*-point grid was used. Simulations were performed under constant pressure allowing both cell volume and shape to change. The electronic self consistent field cut-off criterion was set to 10^{-4} eV and the geometry optimisation cut-off criterion was set to 10^{-3} eV. The cut-off energy was set to 400 eV. A first-order Methfessel-Paxton [18] method was used for smearing of the bands with a width of 0.1 eV. In accordance with the results from Burr *et al*. [7], no Hubbard parameter was applied to the U f-electrons.

In previous work, the solubility of H_2 into U_3Si_2 was investigated [5], highlighting that the reaction was exothermic forming $U_3Si_2H_2$ with an associated swelling of 10 %. In this work, the solubility of H_2 into UB_2 is considered and compared to the previous results in order to help explain the experimentally observed differences in behaviour between UB_2 and U_3Si_2.

H solution onto five interstitial sites was considered:the (0, 0, $\frac{1}{2}$),($\frac{1}{3}$,$\frac{2}{3}$,0) ($\frac{1}{3}$,$\frac{2}{3}$,$\frac{1}{4}$), ($\frac{1}{2}$,0,0) and ($\frac{1}{2}$,$\frac{1}{2}$,$\frac{1}{4}$) sites. The solution enthalpy was considered through the following simple reaction:

$$\frac{1}{2}H_2 \rightarrow H_i \tag{1}$$

The H_2 molecule was modelled as a single dimer in a large cell and the binding energy was found to be in good agreement with the experimental observation (-2.27 eV per atom). The temperature dependent entropy for the H_2 molecule was taken from the NIST-JANAF tables [19].

2.3. Atomic scale modelling of hydrogen in UB_2

To understand the potential improvement related to the addition of UB_2 to U_3Si_2, atomic scale modelling based on density functional theory has been used to assess the propensity for hydrogen solution into UB_2 and compare this behaviour with U_3Si_2. The experimental results suggest that the two main phases do not react with each-other and previous calculations show that the potential for defects resulting from stoichiometry deviations are very low in concentration in the UB_2 system - and it is therefore only necessary to carry out a simple hydrogen solution through interstitial defects computations.

Solution of hydrogen into UB_2 was found to proceed endothermically onto all considered interstitial sites. The lowest solution enthalpy was computed to be 0.81 eV onto the ($\frac{1}{3}$,$\frac{2}{3}$,$\frac{1}{4}$) site. Compared to U_3Si_2, which reacts exothermically with H_2, UB_2 is not expected to accommodate any significant concentration of hydrogen produced as a result of the oxidation of the fuel or the cladding material in the event of cladding failure. In a similar manner to U_3Si_2, increases in temperature are shown to make the solution of H_2 into UB_2 even less favourable as a result of the increasing contribution of the vibrational entropy of the H_2 molecule [5].

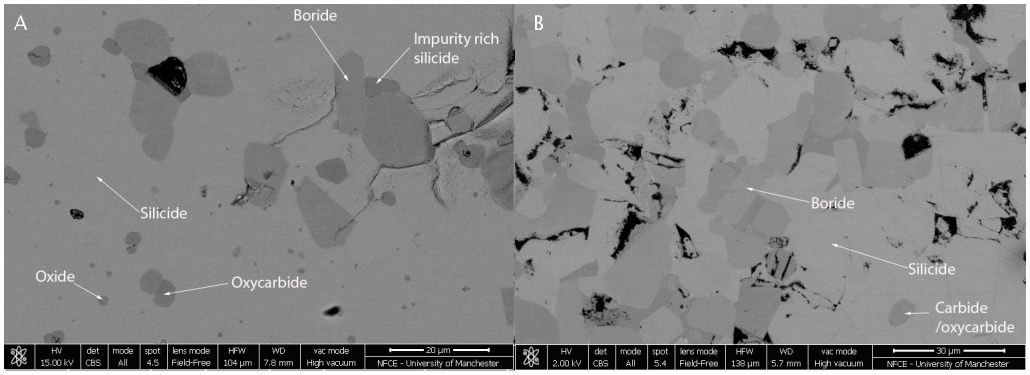

Figure 1: Microstructure of 10wt% (A) and 50wt% (B) UB_2 discs produced using backscatter detector

The volume change associated with a single hydrogen atom entering a 144 atom supercell of UB_2 (0.7 at.%) is 0.2%. Expansion in the a/b-axis is three times larger than in the c-axis indicating a large anisotropy. Given the concentration of hydrogen in solution within the UB_2 lattice is expected to be more than ten orders of magnitude lower than this concentration according to the laws of mass action [20], the volume change as a result of hydrogen incorporation is not expected to be a factor in the degradation of UB_2 when exposed to aqueous environs.

3. Experimental Results

3.1. Microstructure and Phase Analysis

The microstructure of composite pellets and the phases present were examined via electron microscopy and X-ray diffraction (XRD) of powdered pellet sections.

SEM micrographs of a 90 wt.%-10 wt.% and 50 wt.%-50 wt.% U_3Si_2-UB_2 discs are shown in Figure 1 A and B, respectively. Both pellets show UB_2 regions well sintered within a U_3Si_2 matrix. There are also small inclusions of uranium oxide and uranium oxy-carbide within the silicide. From XRD these have been identified as UO_2 and $UC_{0.75}O_{0.25}$. The UCO phase is visible in UB_2 containing samples following milling, while a small mass of U-metal was observed in un-milled UB_2, suggesting the UB_2 was slightly uranium rich following arc melting, and reacted with the carbide milling vessel during powder processing. This phase was identified prior mixing with U_3Si_2, and it is therefore not indicative of a potentially problematic reaction between the UB_2 and U_3Si_2 phases.

Due to both the porosity present within the samples, and the presence of the additional phases, the experimental conclusions drawn from these samples are largely limited to the investigation of interfacial boundary layers between the UB_2 and U_3Si_2 phases. Previous work on burnable poisons in U_3Si_2 has identified that the U_3Si_2 phase can be almost entirely disrupted from small quantities of gadolinium [10]. Analysis of the U_3Si_2 phase following introduction of UB_2 is therefore important to ensure that it remains stable following pressing and sintering.

Energy Dispersive X-ray Spectroscopy (EDX) was employed to determine the microstructural segregation of the two phases (Figure 2). Boride and silicide phases appear distinct according to SEM-EDX analysis.

Although some regions of Ni and Fe impurities exist, and silicon and boron-poor areas are visible, these are not generally co-located at the boundaries between silicide and boride phases.

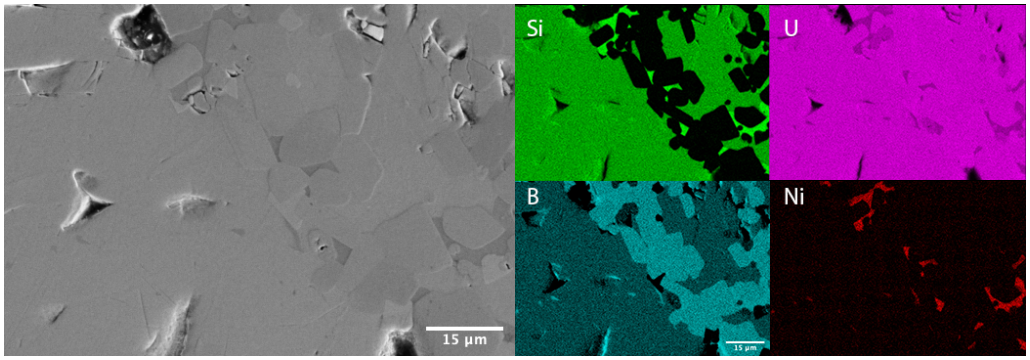

Figure 2: Elemental mapping of 50wt% UB_2 composite pellet, produced from EDX

Ni impurities result from the original source uranium, which was nickel plated and mechanically ground prior to use. Fe contamination likely resulted from pre-crushing of the arc-melted UB_2 material, which was achieved via impact with a steel weight. Both are present in Figure 2 in concentrations less that 0.5 at%. These Impurities appear to cause the formation of silicon-rich silicide regions, although these do not appear to be USi and were not present on XRD analysis.

EDX line-profile analysis of silicide-boride grain boundaries shows a sharp transition between the two phases, up to the resolution of the instrument, suggesting that the phases do not interact at the pellet sintering temperature employed in this study.Some small quantities of uranium metal/uranium carbide/oxycarbide[2] are visible in Figure 2, but these appear to be located very close to larger volumes of impurities and oxide grains. Their formation is not consistently on boride/silicide boundaries. In addition, silicon rich regions visible in Figure 2 are close to the boundary with the UO/UC phases already identified: most likely formed during the preferential oxidation of U over Si. Note that the boron signal visible on Figure 2 within silicon rich regions is a result of the overlapping boron, carbon and uranium peaks present at these X-ray energies, and below a reasonable limit of detection for boron using this technique

Phase analysis was performed via XRD on initial materials, powder mixes and sintered pellets which were crushed prior to analysis. XRD patterns of 50-50 composite material are presented in Figure 3 as representative. The raw UB_2 material produced shows a small quantity of uranium metal present within the material, suggesting that the produced bulk is slightly uranium rich (UB_2 is a line compound [7]), bulk U_3Si_2 appears phase pure. Powder blended material show small quantities (<5%) of uranium oxy-carbide ($UC_{0.75}O_0.25$) and carbide (UC_2 phases), likely resulting from the interaction of uranium metal within the initial boride material reacting with the tungsten carbide milling vessel during the high energy milling process.

4. Discussion

The manufacture of test specimens in the U_3Si_2-UB_2 system suggest that these composite materials are stable during standard cold press and sintering preparations. It is particularly encouraging to note that the UB_2 rich samples produced sintered to similar densities and physical

[2]EDX is unable to distinguish between uranium and carbon due to overlapping low energy peaks, and surface oxygen is overestimated using the technique

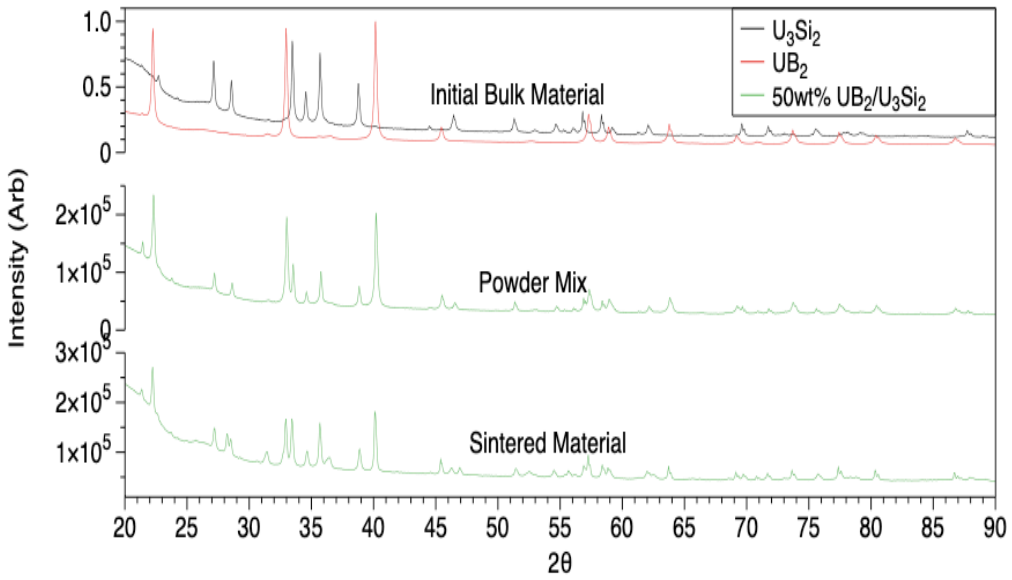

Figure 3: XRD Patterns from initial bulk materials (top), powder blends (middle) and sintered material (bottom). Uranium metal peaks are denoted with an asterisk

robustness as the U_3Si_2 material utilised in the study. A key challenge with employing UB_2 as a monolithic fuel form is expected to be that of sintering; UB_2 has a melting point of over 2400 °C, and similar diboride compounds such as ZrB_2 typically do not fully densify without the use of sintering aids or pressurised sintering techniques [22]. The composites produced here appear to have successfully incorporated UB_2 grains at lower temperatures than are necessary for sintering of pure UB_2. Although several minor phases and inclusions were noted within the material microstructure, the source of these appears to be understood and future studies would likely reduce or remove these via an alternative uranium source and coated steel components.

Modelling of hydrogen solubility within UB_2 demonstrates that the reaction is endothermic and has a predicted volume change of less than 10% of that predicted for U_3Si_2. The inclusion of a UB_2 phase may therefore offer some improvements to the steam performance of U_3Si_2 fuel, without compromising on the improved thermal performance or uranium density which are key drivers of U_3Si_2 development. This will rely on the interaction of the phases within a complex steam environment and detailed experimental data is required to properly assess potential improvements.

The formation of composite fuel pellets is encouraging beyond any potential water performance improvements; UB_2 may be a promising fuel material in its own right, but has historically been considered commercially unattractive due to the need to procure enriched boron for fabrication and as such has been the subject of limited study. Limited modern atomistic modelling studies [6] and historic experimental investigations [23] demonstrate attractive thermal properties for example, and it has a higher uranium density than U_3Si_2 and UO_2. The use of smaller weight percentages of UB_2 within a U_3Si_2 matrix goes some way towards addressing this concern, while arriving at a fuel form which potentially retains the benefit of both materials, and solves the issue

of BA addition to U_3Si_2.

5. Conclusions

Several composite fuel discs were produced, containing a range of U_3Si_2 and UB_2 phases. Despite the incorporation of some impurities and minor phases, the two materials appear to retain phase stability during sintering, and composite material sintering performance was similar to that of reference U_3Si_2 discs produced for this study. The successful incorporation of a boron compound into a U_3Si_2 pellet provides one solution to the need to add burnable absorber material to fuel pellets. Hydrogen solubility in UB_2 is predicted to be low indicating a potential improvement of the material's behaviour when exposed to steam compared to monolithic U_3Si_2.

6. Data Availability

The raw/processed data required to reproduce these findings cannot be shared at this time as the data also forms part of an ongoing study

References

[1] J.M. Harp, P.A. Lessing, B.H. Park, J. Maupin, DOE-NE Report, INL/CON-13-28403 (2013).
[2] F. Cappia, J.M. Harp, J. Nucl. Mater. 518 (2019) 62-79.
[3] E. Sooby-Wood, J.T. White, C.J. Grote, A.T. Nelson, J. Nucl. Mater. 501 (2018) 404-412.
[4] S. Măsková, K. Miliyanchuk, L. Havela, J. Nucl. Mater., 487 (2017) 418-423.
[5] S.C Middleburgh, A. Claisse, D.A. Andersson, R.W. Grimes, P. Olsson, S. Maskova, J. Nucl. Mater. 501 (2018) 234-237.
[6] E. Jossou, L. Malakkal, B. Szpunar, D. Oladimeji, J.A. Szpunar, J. Nucl. Mater. 490 (2017) 41-48.
[7] P.A. Burr, E. Kardoulaki, R. Holmes, S.C. Middleburgh, J. Nucl. Mater. 513 (2019) 45-55.
[8] E. Jossou, D. Oladimeji, L. Malakkal, S. Middleburgh, B. Szpunar, J. Szpunar, J. Nucl. Mater. 494 (2017) 147-156.
[9] S.J.L. Snelgrove, G.L. Hofman, C.L. Trybus, T.C. Wiencek, OSTI Report, DE97001401; NTIS; US Govt. Printing Office Dep (1996).
[10] J.Turner,J. Buckley, G. Phillips, T.J. Abram, J. Nucl. Mater., 509 (2018) 204-211.
[11] S.C. Middleburgh, R.W. Grimes, K.H. Desai, P.R. Blair, L. Hallstadius, K. Backman, P. Van Uffelen, J. Nucl. Mater., 427 (2012) 359-363.
[12] G. Kresse and J. Hafner. Ab initio molecular dynamics for liquid metals. Phys. Rev. B, 47:558, 1993.
[13] G. Kresse and J. Hafner. Ab initio molecular-dynamics simulation of the liquid-metal-amorphous-semiconductor transition in germanium. Phys. Rev. B, 49:14251, 1994.
[14] G. Kresse and J. Furthmller. Efficiency of ab-initio total energy calculations for metals and semiconductors using a plane-wave basis set. Comput. Mat. Sci., 6:15, 1996.
[15] P. E. Blochl. Projector augmented-wave method. Phys. Rev. B, 50:17953, 1994.
[16] J. P. Perdew, K. Burke, and M. Ernzerhof. Generalized gradient approximation made simple. Phys. Rev. Lett., 77:3865, 1996.
[17] S.C. Middleburgh, D.C. Parfitt, P.R. Blair, R.W. Grimes, J. Am. Ceram. Soc. (2011) 94 2225-2229.
[18] M. Methfessel, A. Paxton, Phys. Rev. B 40 (1989) 3616-3621.
[19] M.W. Chase Jr., C.A. Davies, J.R. Downey Jr., D.J. Frurip, R.A. McDonald, A.N. Syverud, NIST JANAF Thermochemical Tables (1985) 20899,
[20] A. Chroneos, R.W. Grimes, Appl. Phys. Lett., 91 (2007) 192106.
[21] J.M Harp, P.A. Lessing, R. E. Hoggan, J. Nucl. Mater., 466 (2015) 728-738
[22] Chamberlain, A. L., Fahrenholtz, W. G., Hilmas, G. E., J. Am. Ceram. Soc., 89 (2006) 450-456
[23] Flotow, H. E., Osborne, D. W., OHare, P. A. G., Settle, J. L., Mrazek, F. C., Hubbard, W. N., The Journal of Chemical Physics, 51(2) (1969), 583592.